Electronic Supplementary Material (ESI) for RSC Advances.

Supporting Information for the Manuscript Entitled

Multiresponsive Micellar Block Copolymers from 2-Vinylpyridine and Dialkylvinylphosphonates with a Tunable Lower Critical Solution Temperature

Friederike Adams, Peter T. Altenbuchner*, Patrick D. L. Werz, and Bernhard Rieger*

WACKER-Lehrstuhl für Makromolekulare Chemie, Technische Universität München, Lichtenbergstraße 4, 85747 Garching b. München, Germany.

Table of Contents

1. Experimental procedure 2

2. Polymerization results 5

3. Characterization of micelles 11

Experimental procedure

Materials and Methods.

All reactions were carried out under argon atmosphere using standard Schlenk or glovebox techniques. All glassware was heat dried under vacuum prior to use. Unless otherwise stated, all chemicals were purchased from Sigma-Aldrich, Acros Organics, or ABCR and used as received. Toluene, thf, diethylether dichloromethane and pentane were dried using a MBraun SPS-800 solvent purification system. Hexane was dried over 3 Å molecular sieves. Compound $Y(CH_2Si(CH_3)_3)_3(thf)_2$, $LiCH_2TMS$ and catalyst 1 are prepared according to literature procedures.[1-4] Monomers 2-vinylpyridine (2VP) and the dialkyl vinyl phosphonates (DAVP) were dried over calcium hydride and distilled prior to use.
NMR spectra were recorded on a Bruker AVIII-300 and AVIII-500 Cryo spectrometer. Unless otherwise stated, ^1H- and ^{13}C-NMR spectroscopic chemical shifts δ are reported in ppm relative to the residual proton signal of the solvent. δ (^1H) is calibrated to the residual proton signal, δ (^{13}C) to the carbon signal of the solvent. Unless otherwise stated, coupling constants J are averaged values and refer to couplings between two protons. Deuterated solvents were obtained from Sigma-Aldrich and dried over 3 Å molecular sieves.

Copolymerization Procedures.

After dissolving the calculated amount of catalyst in dichloromethane at room temperature, the respective equivalents of 2-vinylpyridine were added in one portion. The reaction mixture was stirred for 90 minutes. One aliquot (0.1 mL) was taken and quenched by the addition of 0.4 mL CD_3OD (calculation of conversion of 2-vinylpyridine via ^1H-NMR) while the calculated amount of a second monomer (or mixture of two dialkyl vinyl phosphonates) was added to the reaction solution, stirred over night and quenched by addition of 0.5 mL methanol. Before quenching an aliquot (0.1 mL) is, once again, taken and quenched with 0.5 mL CD_3OD to calculate the conversion of vinylphosphonates via ^{31}P-NMR-spectroscopy. The polymers were precipitated by addition of the reaction mixtures to pentane (150 mL) and decanted from solution. Residual solvent was removed by freeze-drying from benzene or water (100 mL) over night. The polymer of the aliquot of the first polymerization-sequence is dried under vacuum at 60 °C overnight.

Characterization of Polymer Samples.

Molecular-weights and molecular-weight-distributions of the first polymerization sequence are measured via GPC-MALS analysis of the first aliquot. Ratio of A/B [2VP/DAVP] is calculated via ^1H-NMR-spectroscopy of the dried blockcopolymer. The molecular-weight of the blockcopolymer is determined through the ratio of A/B and the molecular weight of the first block (A). Molecular-weight-distributions are measured via GPC-MALS analysis.

Gel permeation chromatography (GPC) was carried out with samples of 5 mg/mL concentration on a Varian LC-920 equipped with two PL Polargel columns. As eluent a mixture of THF/water (1:1; v:v), 9 g/L tetrabutylammonium bromide (TBAB) and 680 mg/L_{THF} 3,5-di-tert-butyl-4-hydroxytoluene (BHT) was used. Absolute molecular weights have been determined online by multiangle light scattering (MALS) analysis using a Wyatt Dawn Heleos II in combination with a Wyatt Optilab rEX as concentration source.

Lower critical solution temperature (LCST)-measurements were carried out on a Cary 50 UV−Vis spectrophotometer from Varian. The LCST was determined by spectrophotometric detection of the changes in transmittance at λ = 500 nm of the aqueous polymer solutions. The heating/cooling rate was 1.0 K/min in steps of 1 K followed by a 5 min period of constant temperature to ensure equilibration. For determination of the transition hysteresis, equilibration periods of 3, 1.5, 0.75, 0.5, and 0.25 min or no equilibration period was used. The cloud point was defined as the temperature corresponding to a 10% decrease in optical transmittance.

Preparation of Micelles

To obtain Nile red-loaded micelles, firstly Nile red was dissolved in DMSO (c= 0.3 mg/mL). Under continuous stirring the Nile red solution was added dropwise to the freshly prepared blank-micelle solution (Micelle/Nile-Red = 1/10). The mixture was then stirred for 1 hour followed by overnight dialysis against water (MWCO: 6000 – 8000). Afterwards non-encapsulated Nile red was removed by an additional centrifugation step at 4000 rpm for 10 min at room temperature. The supernatant was transferred into a new reaction tube.

TEM images

High-resolution transmission electron microscopy (TEM) was performed on a JEOL JEM100CX using an accelerating voltage of 100 kV. Samples were prepared from a dilute aqueous solution using a 2% uranyl acetate solution as the negative stain.
TEM images were prepared from aqueous solution of the micelles on a copper tape and dried until the water disappeared and measured immediately.

Ligand synthesis.

$H_2(ONOO)^{tBu}$ [5]

A solution of 2.0 equivalents of 2,4-di-tert-butylphenol, 1.0 equivalents 2-methoxyethylamine and aqueous formaldehyde-solution (36% in water; 3.0 eq.) in methanol were refluxed for 10 days. The mixture was cooled and the colorless solid was separated via filtration. After double recrystallization from ethanol the product is yielded as colorless crystals.

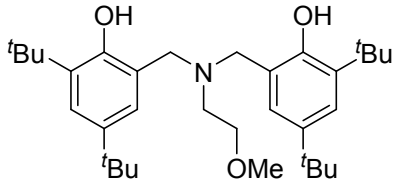

$C_{33}H_{53}NO_3$
M: 511.79

$H_2(ONOO)^{tBu}$

Yield: 45% (colorless crystals)

^{1}H-NMR (300 MHz, $CDCl_3$, 300 K): δ (ppm) = 8.52 (s, 2H, O*H*), 7.21 (d, ^4J = 2.5 Hz, 2H, H_{arom}), 6.88 (d, ^4J = 2.5 Hz, 2H, H_{arom}), 3.74 (s, 4H, $ArCH_2$), 3.56 (t, ^3J = 5.1 Hz, 2H, $H_{sidearm}$), 3.47 (s, 3H, O*Me*), 2.75 (t, ^3J = 5.1 Hz, 2H, $H_{sidearm}$), 1.41 (s, 18H, ^{t}Bu), 1.27 (s, 18H, ^{t}Bu).

^{13}C-NMR (75 MHz, $CDCl_3$, 300 K): δ (ppm) = 153.0, 140.8, 136.1, 125.0, 123.5, 121.7, 71.5, 58.9, 58.2, 51.5, 35.1, 34.2, 31.8, 29.7.

Complex synthesis.

$(ONOO)^{tBu}Y(CH_2TMS)(thf)$(1) [6]

One equivalent of proligand $H_2(ONOO)^{tBu}$ in toluene is added to a stirred solution of $Y(CH_2Si(CH_3)_3)_3(thf)_2$ in pentane at 0 °C. The resulting solution is stirred overnight at room temperature. The solvent is removed *in vacuo* and the resulting solid is washed and recrystallized from pentane.

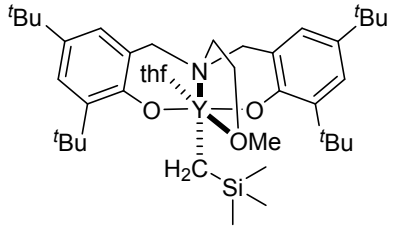

$C_{41}H_{70}NO_4SiY$
M: 758.00

Yield: 43% (colorless powder)

^{1}H-NMR (300 MHz, C_6D_6, 300 K): δ (ppm) = 7.61 (d, ^4J = 2.6 Hz, 2H, H_{arom}), 7.09 (d, ^4J = 2.6 Hz, 2H, H_{arom}), 4.00 – 3.89 (m, 4H, H_{THF}), 3.78 (d, ^2J = 12.4 Hz, 2H, $ArCH_2$), 2.89 (d, ^2J = 12.4 Hz, 2H, $ArCH_2$), 2.78 (s, 3H, O*Me*), 2.42 (t, ^3J = 5.4 Hz, 2H, $H_{sidearm}$), 2.20 (t, ^3J = 5.4 Hz, 2H, $H_{sidearm}$), 1.81 (s, 18H, ^{t}Bu), 1.46 (s, 18H, ^{t}Bu), 1.19 – 1.11 (m, 4H, H_{THF}), 0.52 (s, 9H, H_{TMS}), -0.38 (d, $^2J_{Y,H}$ = 3.3 Hz, 2H, CH_2TMS).

^{13}C-NMR (126 MHz, C_6D_6, 300 K): δ (ppm) = 161.6 (d, $^2J_{C,Y}$ = 1.8 Hz), 136.8, 136.6, 125.6, 124.4, 124.1, 74.0, 71.7, 64.9, 61.3, 49.3, 35.6, 34.3, 32.3, 30.3, 25.4, 25.1, 4.9.

1. Polymerization results

GPC traces.

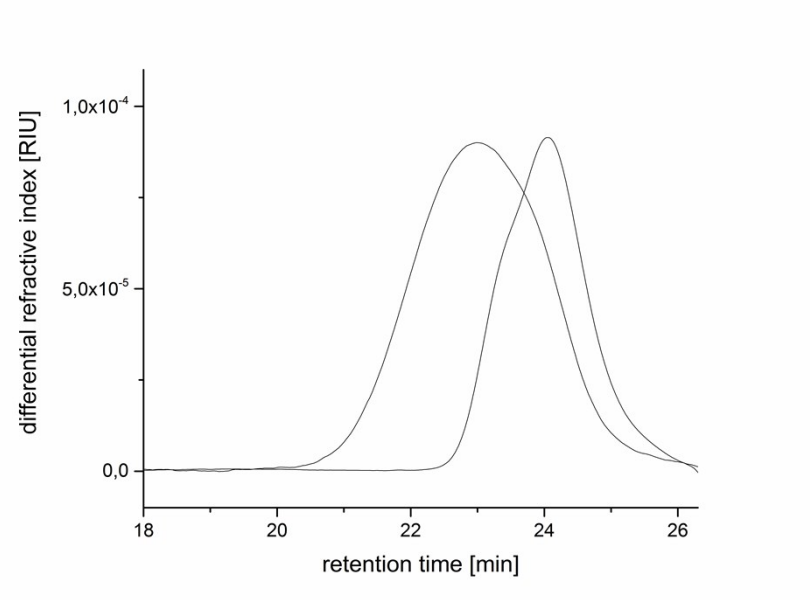

Figure S 1: GPC-traces of blockcopolymer AB ($2VP_{100}/DEVP_{100}$; entry 1, table 1).Right: P2VP Homopolymer before addition of Block B. Left: Blockcopolymer.

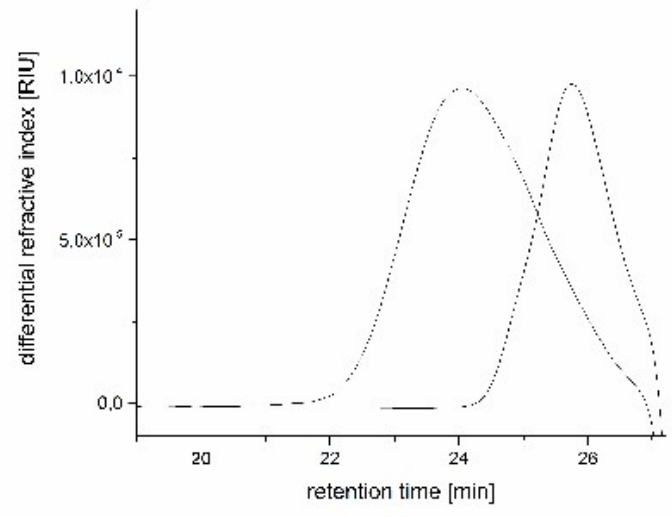

Figure S 2: GPC-traces of Blockcopolymer AB ($2VP_{50}/DEVP_{50}$; entry 2, table 1). Right: P2VP Homopolymer before addition of Block B. Left: Blockcopolymer.

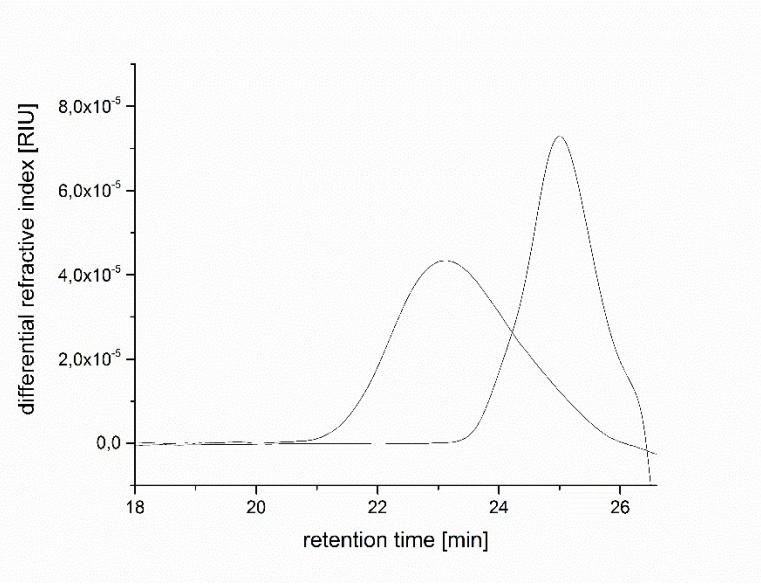

Figure S 3: GPC-traces of blockcopolymer AB ($2VP_{50}/DEVP_{90}$; entry 3, table 1). Right: P2VP Homopolymer before addition of Block B. Left: Blockcopolymer.

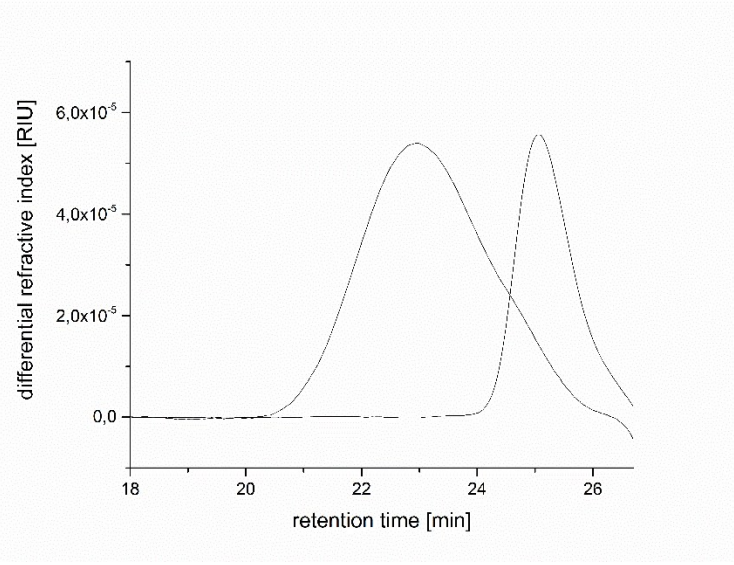

Figure S 4: GPC-traces of blockcopolymer AB ($2VP_{50}/DEVP_{120}$; entry 4, table 1). Right: P2VP Homopolymer before addition of Block B. Left: Blockcopolymer.

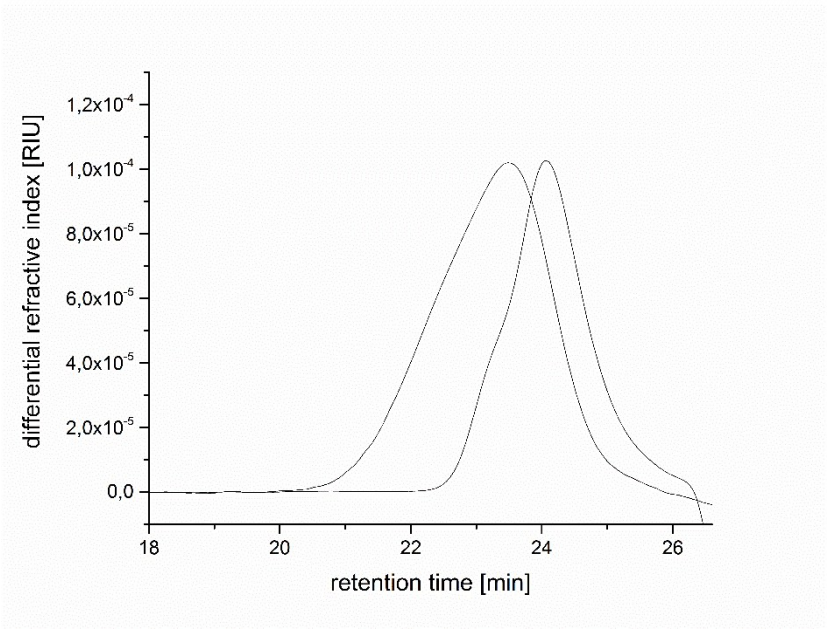

Figure S 5: GPC-traces of blockcopolymer ABB' ($2VP_{100}/DEVP_{97}/DPVP_3$; entry 6, table 1). Right: P2VP Homopolymer before addition of Block B. Left: Blockcopolymer.

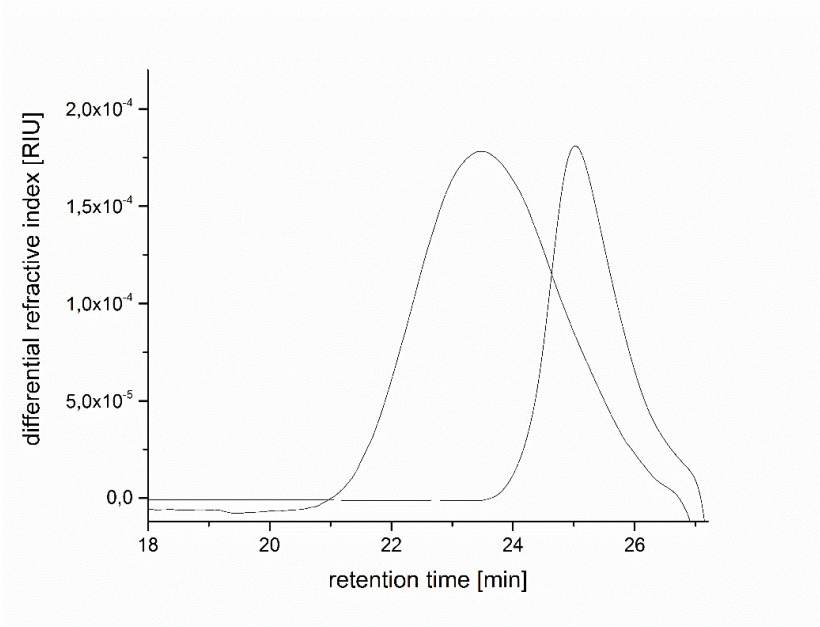

Figure S 6: GPC-traces of blockcopolymer ABB' ($2VP_{100}/DEVP_{90}/DMVP_{10}$; entry 7, table 1). Right: P2VP Homopolymer before addition of Block B. Left: Blockcopolymer.

Blockcopolymers.

Exemplary for all AB-blockcopolymers:

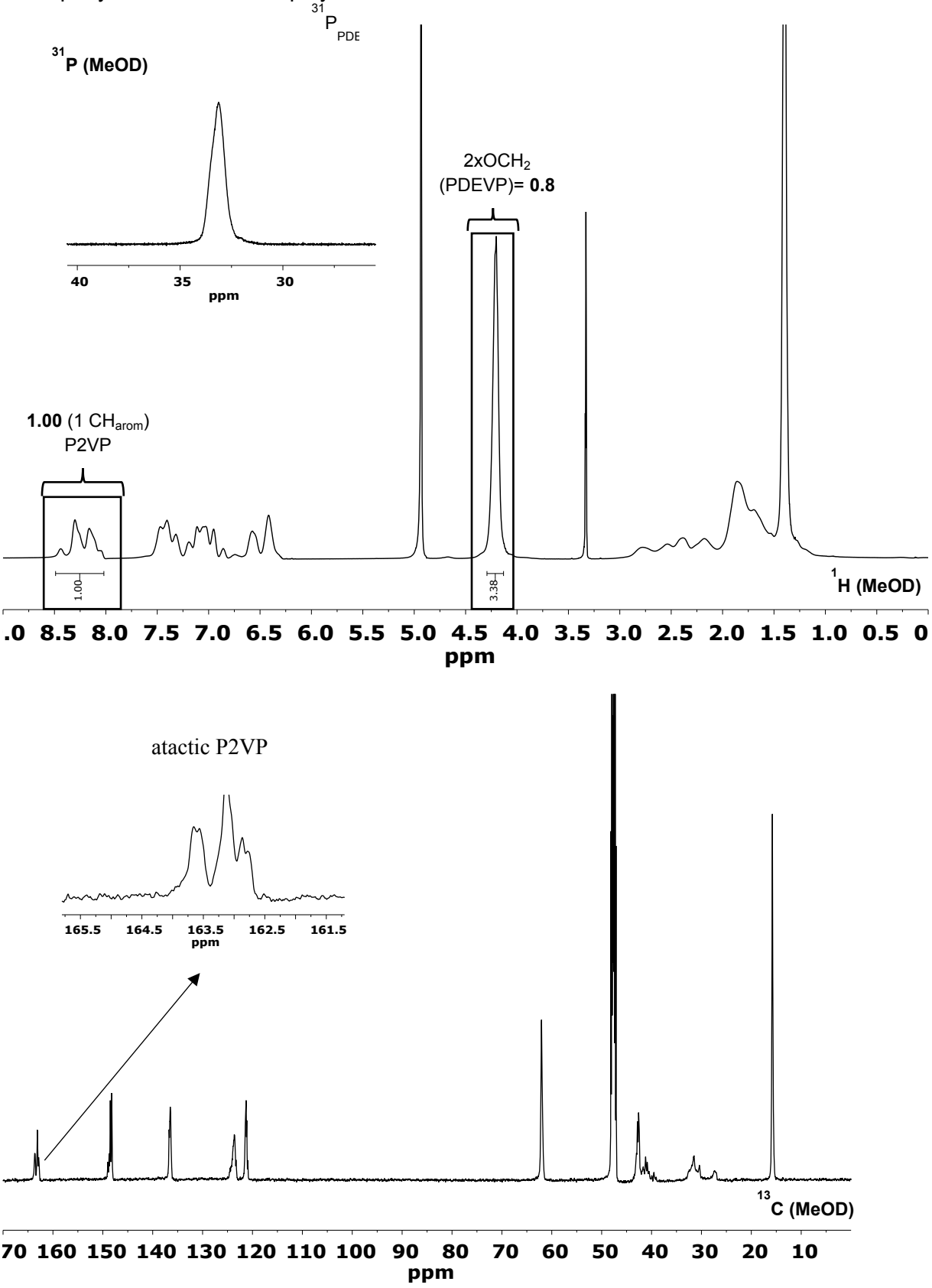

Figure S 7: ^{1}H-, ^{31}P- and^{13}C-NMR spectrum of AB ($2VP_{100}/DEVP_{100}$; entry 1, table 1) in MeOD at 298 K.

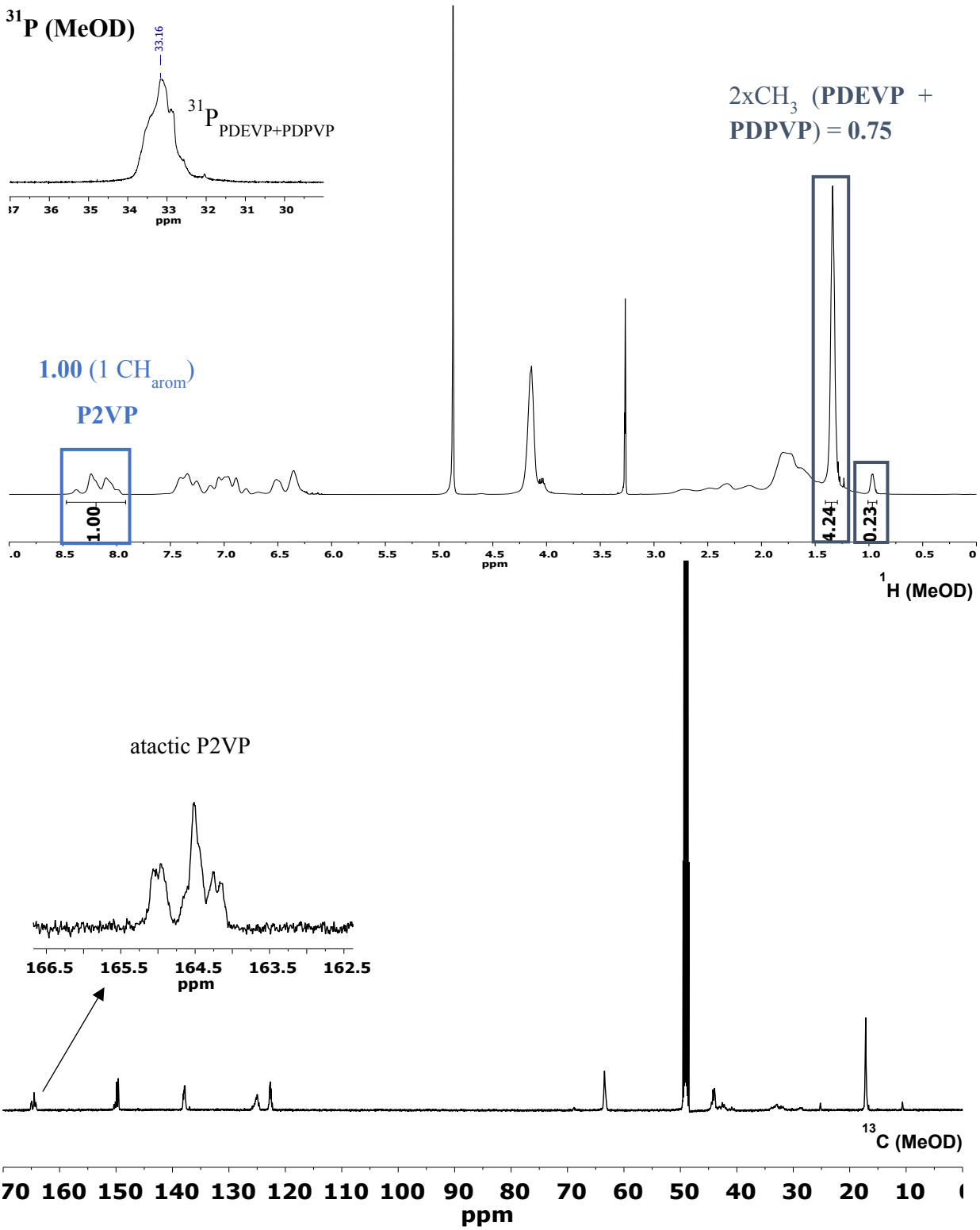

Figure S 8: ^{1}H-, ^{31}P- and ^{13}C-NMR spectrum of ABB' ($2VP_{100}/DEVP_{90}/DPVP_{10}$; entry 6, table 1) in MeOD at 298 K. Assignment of the Protons according to *Rieger et al.* Overlapping of PDEVP and PDPVP-^{31}P-signal. [7]

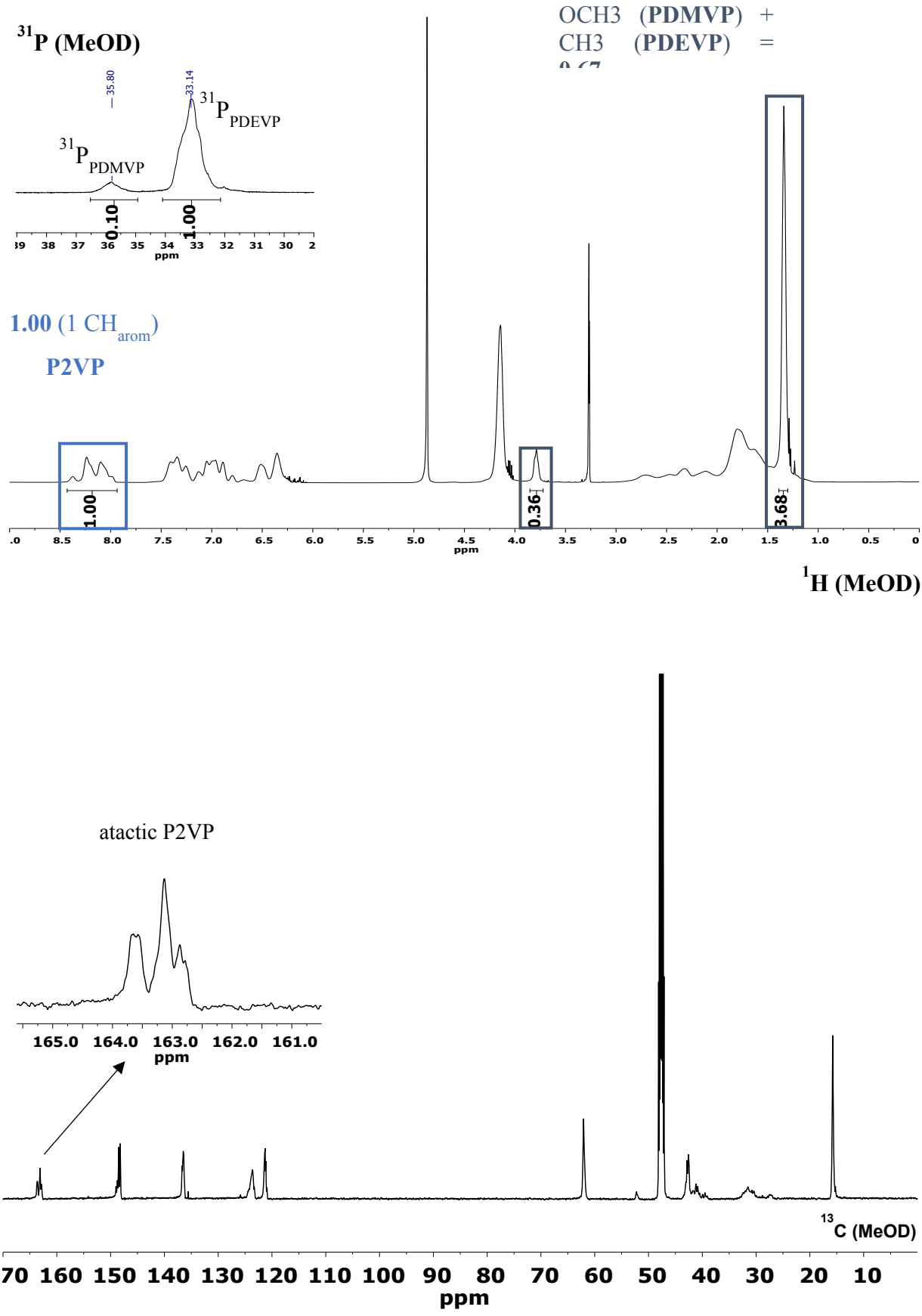

Figure S 9: ^{1}H-, ^{31}P- and ^{13}C-NMR spectrum of ABB' ($2VP_{100}/DEVP_{90}/DMVP_{10}$; entry 8 table 1) in MeOD at 298 K. Assignment of the Protons according to Rieger et al.[7]

2. Characterization of micelles

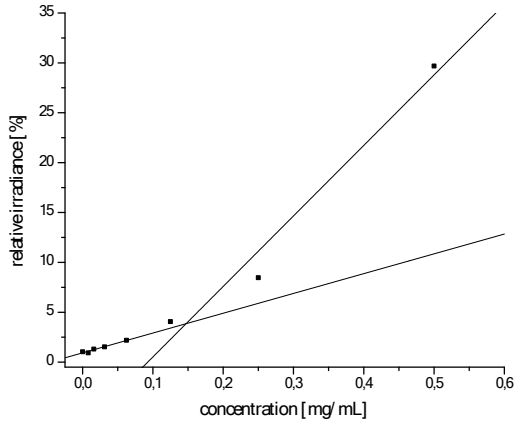

Figure S 10: Determination of critical micelle concentration (CMC) with Nile red for AB ($2VP_{100}/DEVP_{100}$; entry 1 table 1).

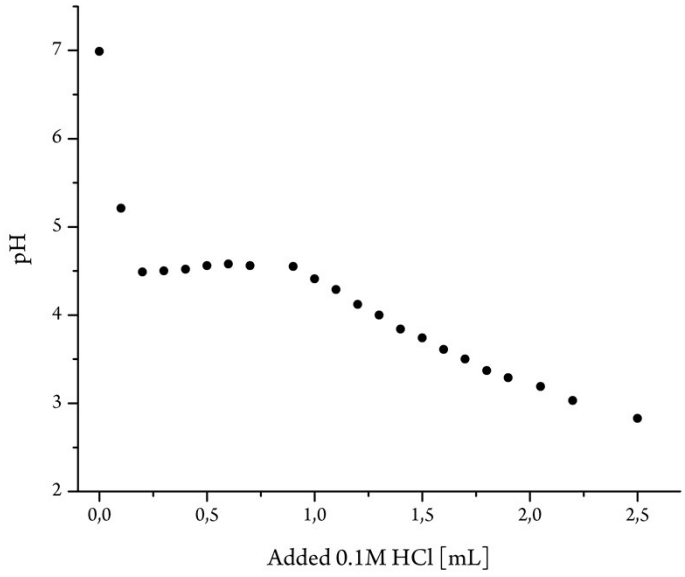

Figure S 11: Titrationcurve of AB_1 ($2VP_{100}/DEVP_{100}$; entry 1 table 1) with 0.1 M hydrogenchloride-solution.

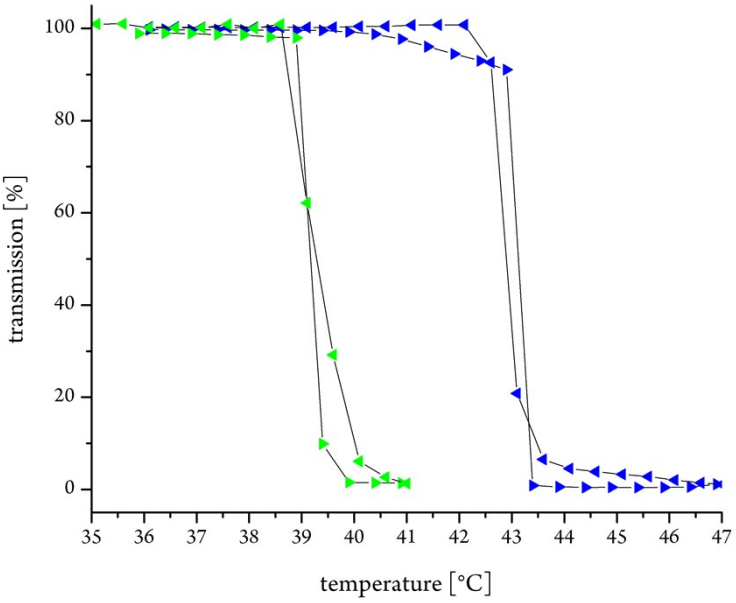

Figure S 12: LCST-UV/VIS-measurement of blockcopolymer AB[1] ($2VP_{100}/DEVP_{100}$; entry 1 table 1). The cloud point was determined at 10% decrease of transmittance for 2.5 wt % aqueous polymer solution (blue: deionized, green: PBS puffer).

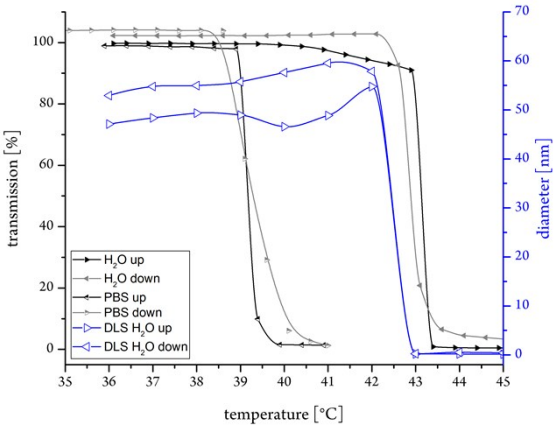

Figure S 13: LCST-UV/VIS-measurement and DLS-measurement of blockcopolymer AB[1] ($2VP_{100}/DEVP_{100}$; entry 1 table 1) in H_2O and PBS buffer solution.

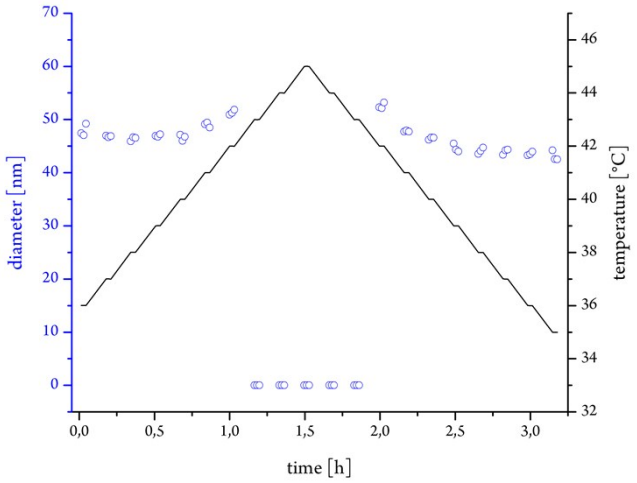

Figure S 14: LCST-DLS-measurement of blockcopolymer AB[1] ($2VP_{100}/DEVP_{100}$; entry 1 table 1).

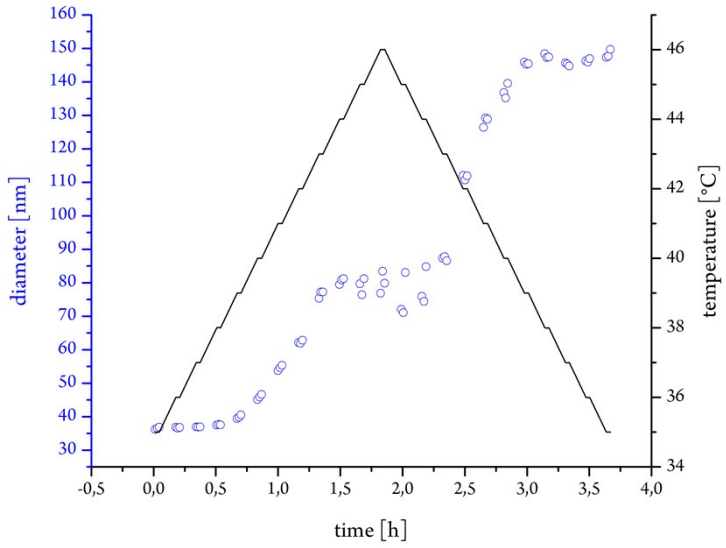

Figure S 15: LCST-DLS-measurement of blockcopolymer AB[2] ($2VP_{50}/DEVP_{50}$; entry 2 table 1).

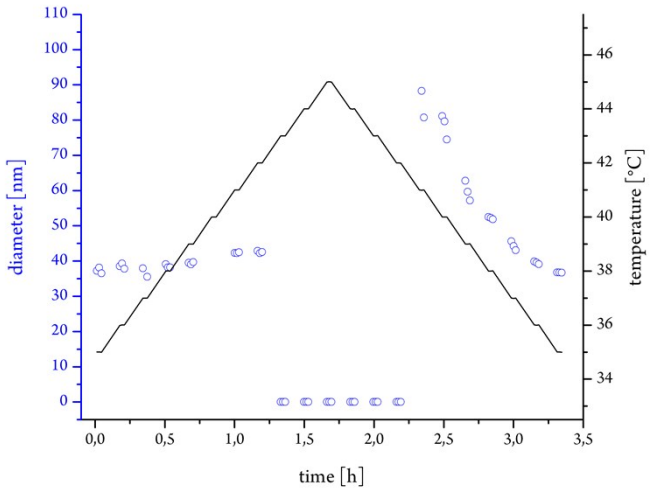

Figure S 16: LCST-DLS-measurement of blockcopolymer AB^3 ($2VP_{50}/DEVP_{90}$; entry 3 table 1).

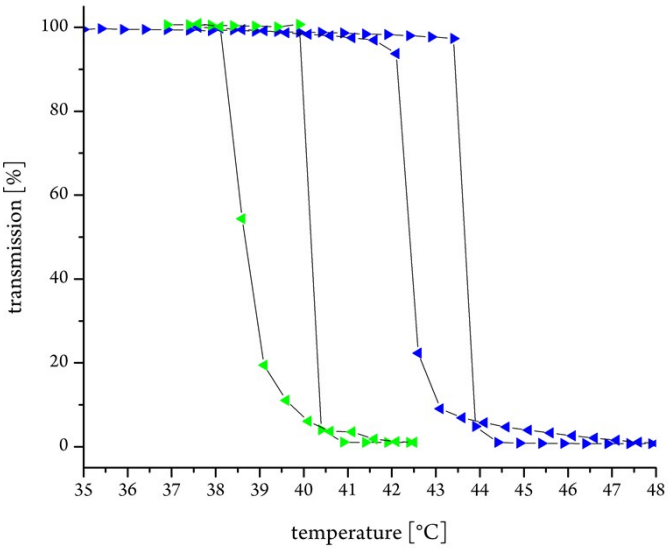

Figure S 17: LCST-UV/VIS-measurement of blockcopolymer AB^3 ($2VP_{50}/DEVP_{90}$; entry 3 table 1). The cloud point was determined at 10% decrease of transmittance for 2.5 wt % aqueous polymer solution (blue: deionized, green: PBS puffer).

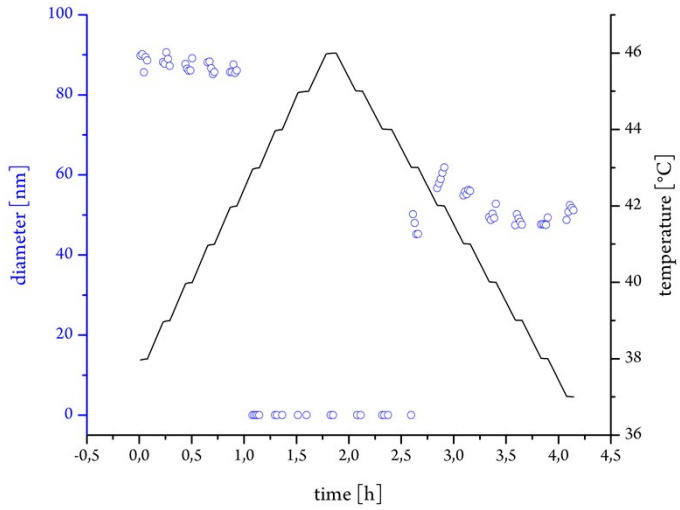

Figure S 18: LCST-DLS-measurement of blockcopolymer AB^4 ($2VP_{50}/DEVP_{120}$; entry 4 table 1).

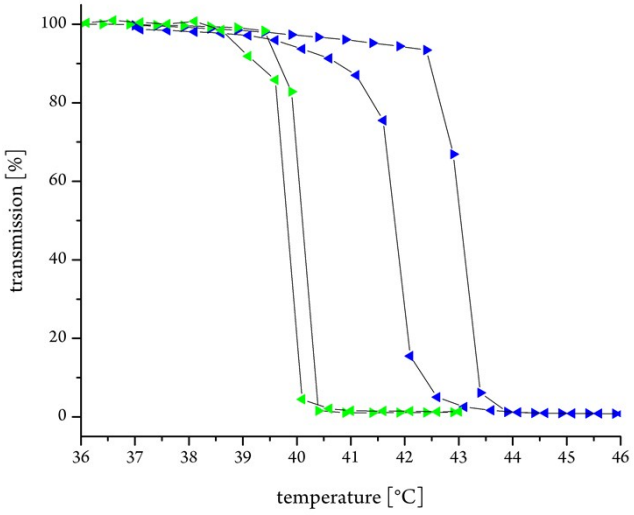

Figure S 19: LCST-UV/VIS-measurement of blockcopolymer AB^4 ($2VP_{50}/DEVP_{120}$; entry 4 table 1). The cloud point was determined at 10% decrease of transmittance for 2.5 wt % aqueous polymer solution (blue: deionized, green: PBS puffer).

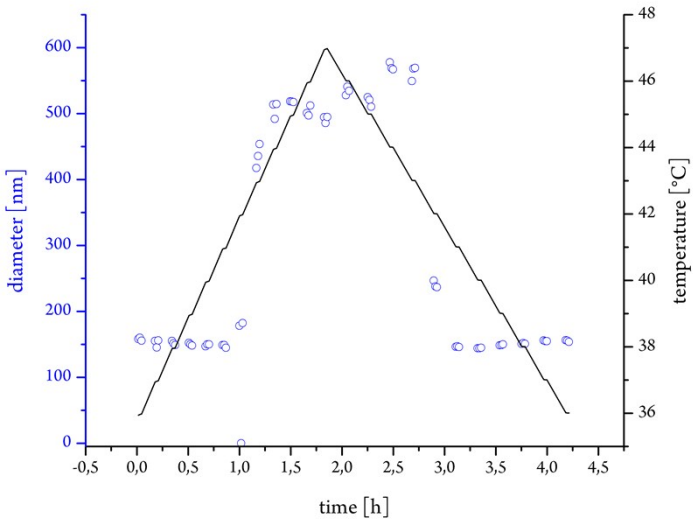

Figure S 20: LCST-DLS-measurement of blockcopolymer AB[5] ($2VP_{200}/DEVP_{200}$; entry 5 table 1).

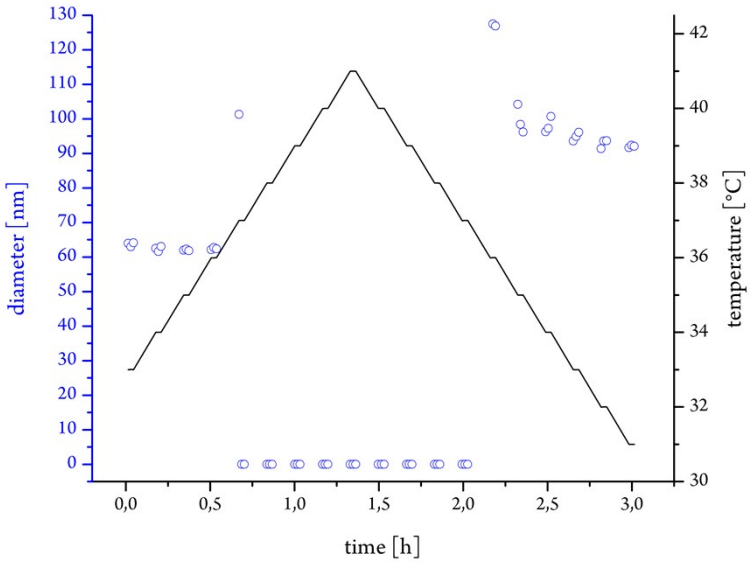

Figure S 21: LCST-DLS-measurement of blockcopolymer ABB'[1] ($2VP_{100}/DEVP_{90}/DPVP_{10}$; entry 6, table 1).

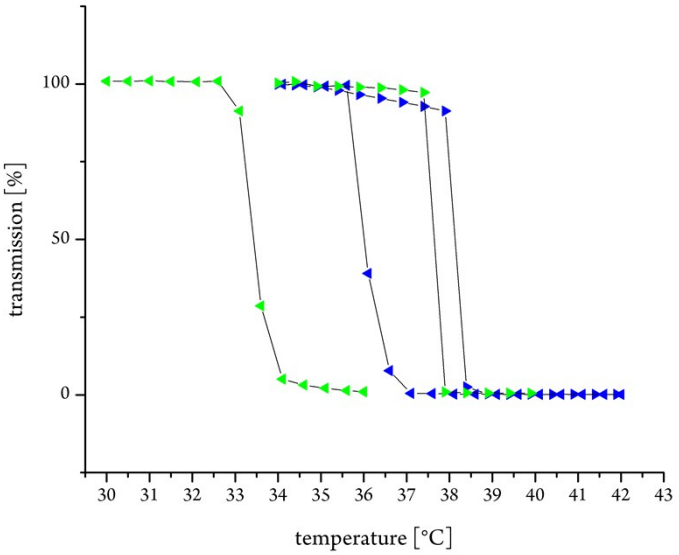

Figure S 22: LCST-UV/VIS-measurement of blockcopolymer ABB'[1] ($2VP_{100}/DEVP_{90}/DPVP_{10}$; entry 6, table 1).The cloud point was determined at 10% decrease of transmittance for 2.5 wt % aqueous polymer solution (blue: deionized, green: PBS puffer).

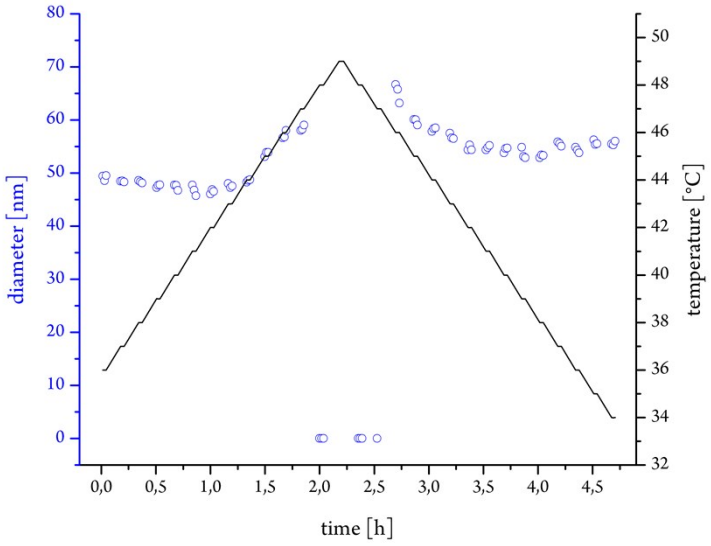

Figure S 23: LCST-DLS-measurement of blockcopolymer ABB'[2] ($2VP_{100}/DEVP_{90}/DMVP_{10}$; entry 7, table 1).

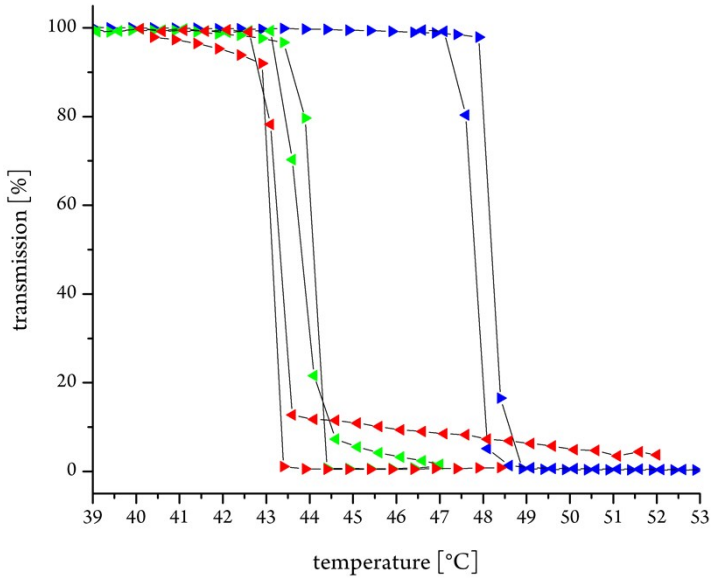

Figure S 24: LCST-UV/VIS-measurement of blockcopolymer ABB'[2] ($2VP_{100}/DEVP_{90}/DMVP_8$; entry 7, table 1).The cloud point was determined at 10% decrease of transmittance for 2.5 wt % aqueous polymer solution (blue: deionized, green: PBS puffer, red: DMEM puffer).

1. Altenbuchner, P. T.; Soller, B. S.; Kissling, S.; Bachmann, T.; Kronast, A.; Vagin, S. I.; Rieger, B., *Macromolecules* **2014,** *47* (22), 7742-7749.
2. Hultzsch, K. C.; Voth, P.; Beckerle, K.; Spaniol, T. P.; Okuda, J., *Organometallics* **2000,** *19* (3), 228-243.
3. Vaughn, G. D.; Krein, K. A.; Gladysz, J. A., *Organometallics* **1986,** *5* (5), 936-42.
4. Cai, C.-X.; Toupet, L.; Lehmann, C. W.; Carpentier, J.-F., *J. Organomet. Chem.* **2003,** *683* (1), 131-136.
5. Tshuva, E. Y.; Groysman, S.; Goldberg, I.; Kol, M.; Goldschmidt, Z., *Organometallics* **2002,** *21* (4), 662-670.
6. Amgoune, A.; Thomas, C. M.; Roisnel, T.; Carpentier, J.-F., *Chem. Eur. J.* **2005,** *12* (1), 169-79.
7. Zhang, N.; Salzinger, S.; Rieger, B., *Macromolecules* **2012,** *45* (24), 9751-9758.